Photochemical & Photobiological Sciences

Accepted Manuscript

This is an *Accepted Manuscript*, which has been through the Royal Society of Chemistry peer review process and has been accepted for publication.

Accepted Manuscripts are published online shortly after acceptance, before technical editing, formatting and proof reading. Using this free service, authors can make their results available to the community, in citable form, before we publish the edited article. We will replace this *Accepted Manuscript* with the edited and formatted *Advance Article* as soon as it is available.

You can find more information about *Accepted Manuscripts* in the Information for Authors.

Please note that technical editing may introduce minor changes to the text and/or graphics, which may alter content. The journal's standard Terms & Conditions and the Ethical guidelines still apply. In no event shall the Royal Society of Chemistry be held responsible for any errors or omissions in this *Accepted Manuscript* or any consequences arising from the use of any information it contains.

ROYAL SOCIETY OF CHEMISTRY

www.rsc.org/pps

TABLE OF CONTENTS ENTRY

Cloning, overexpression in a heterologous host, and functional characterisation of the first CPD-Class I photolyase from a UV-resistant strain isolated from a high altitude hypersaline lake in Argentinean Puna provide strong support for the involvement of this extremoenzyme in the formerly observed high photoreactivation ability of the extremophilic *Acinetobacter*.

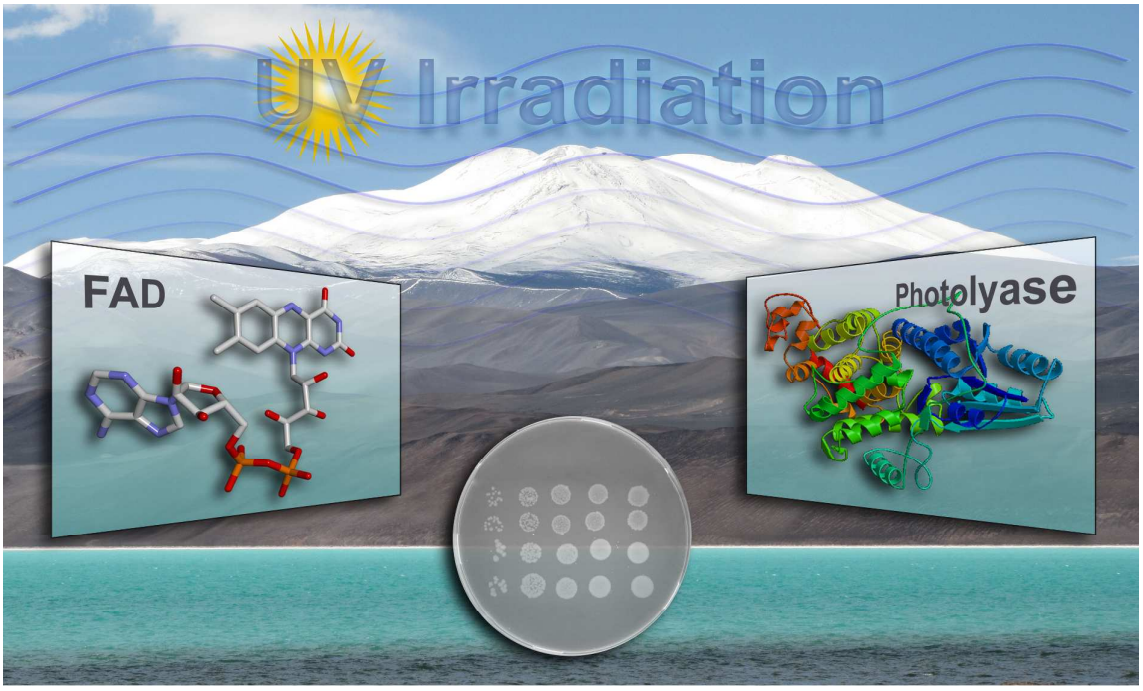

First characterisation of a CPD-Class I photolyase from an UV-resistant extremophile isolated from High-Altitude Andean Lakes

Virginia Helena Albarracín[*1,2,3], Julian Simon[3], Gopal P. Pathak[3], Lorena Valle[4], Thierry Douki[5], Jean Cadet[5], Claudio Darío Borsarelli[4], María Eugenia Farias[1] and Wolfgang Gärtner[3*]

[1]Planta Piloto de Procesos Industriales y Microbiológicos (PROIMI), CCT, CONICET. Av. Belgrano y Pasaje Caseros. 4000- S. M. de Tucumán, Argentina.

[2]Facultad de Ciencias Naturales e Instituto Miguel Lillo, Universidad Nacional de Tucumán. 4000 Tucumán, Argentina.

[3]Max-Planck-Institute for Chemical Energy Conversion, Stiftstrasse 34-36, D-45470 Mülheim, Germany.

[4]Centro de Investigaciones y Transferencia de Santiago del Estero (CITSE), CONICET, Universidad Nacional de Santiago del Estero, RN 9, Km 1125. 4206 – Santiago del Estero, Argentina.

[5]Laboratoire "Lésions des Acides Nucléiques" INaC/SCIB UMR-E3 CEA-UJF/CEA-Grenoble, 17 avenue des Martyrs, 38054 Grenoble Cedex 9, France

Running headline: CPD photolyase from an UV-resistant extremophile

Key words: *Acinetobacter*, extremophiles, High-Altitude Andean Lakes, photolyase, UV-resistance, DNA repair

***Corresponding authors**:

Virginia Helena Albarracín, virginia-helena.albarracin@cec.mpg.de

Planta Piloto de Procesos Industriales y Microbiológicos (PROIMI), CCT, CONICET. Av. Belgrano y Pasaje Caseros. 4000- S. M. de Tucumán, Argentina. Tel: 0054-381-4344888 Int. 35. Fax: 0054-381-4344887.

Wolfgang Gärtner, wolfgang.gaertner@cec.mpg.de

TABLE OF CONTENTS ENTRY

Cloning, overexpression in a heterologous host, and functional characterisation of the first CPD-Class I photolyase from a UV-resistant strain isolated from a high altitude hypersaline lake in Argentinean Puna provide strong support for the involvement of this extremoenzyme in the formerly observed high photoreactivation ability of the extremophilic *Acinetobacter*.

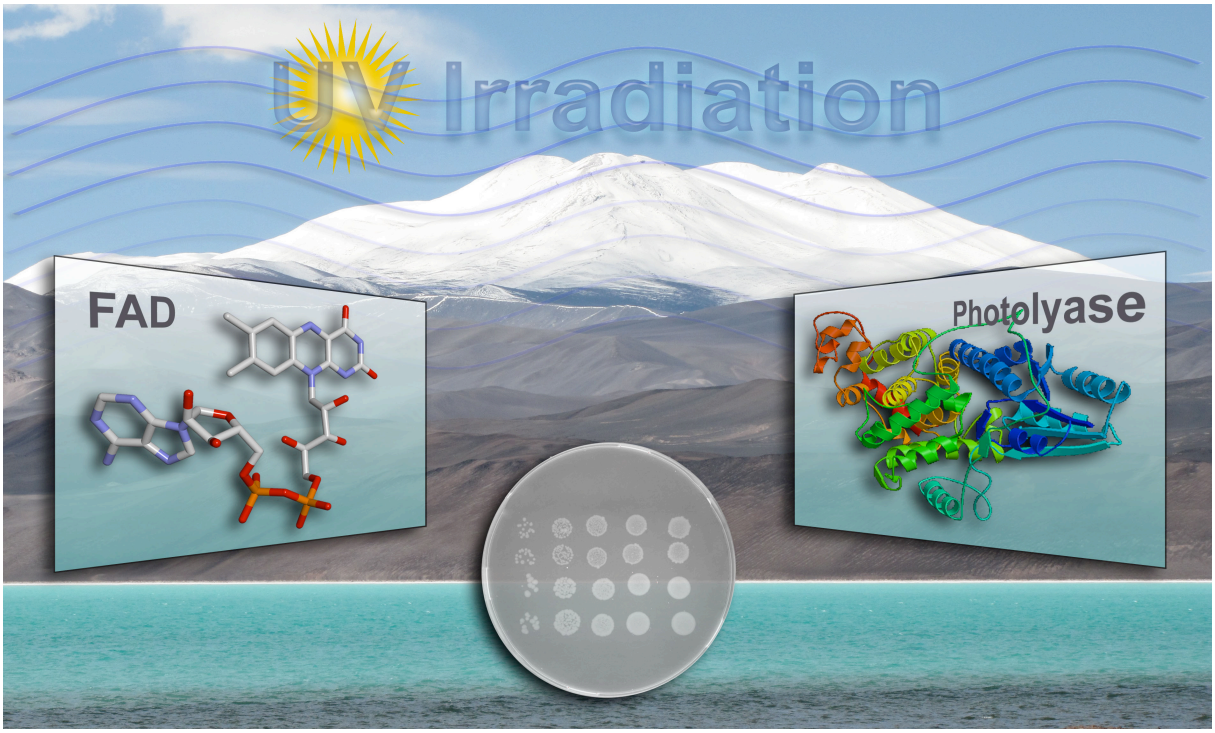

ABSTRACT

UV-resistant *Acinetobacter* sp. Ver3 isolated from High-Altitude Andean Lakes (HAAL) in Argentinean Puna, one of the highest UV exposed ecosystems on Earth, showed efficient DNA photorepairing ability, coupled to highly efficient antioxidant enzyme activities in response to UV-B stress. We herein present the cloning, expression, and functional characterization of a cyclobutane pyrimidine dimer (CPD)-Class I photolyase (Ver3Phr) from this extremophile to prove its involvement in the previously noted survival capability. Spectroscopy of the overexpressed and purified protein identified a flavin adenin dinucleotide (FAD) and 5,10-methenyltetrahydrofolate (MTHF) as chromophore and antenna molecules, respectively. All functional analyses were performed in parallel with the ortholog *E. coli* photolyase. Whereas the *E. coli* enzyme showed the FAD chromophore as a mixture of oxidised and reduced state, the Ver3 chromophore always remained partly (including the semiquinone state) or fully reduced under all experimental conditions tested. Functional complementation of Ver3Phr in Phr$^-$-RecA *E.coli* strains was assessed by traditional UFC counting and measurement of DNA bipyrimidine photoproducts by HPLC coupled with electrospray ionisation-tandem mass spectrometry (ESI-MS/MS) detection. The results identified strong photoreactivation ability *in vivo* of Ver3Phr while its nonphotoreactivation function, probably related with the stimulation of nucleotide excision repair (NER), was not as manifest as for EcPhr. Whether this is a question of the approach using an exogenous photolyase incorporated in a non-genuine host or a fundamental different behaviour of a novel enzyme from an exotic environment will need of further studies.

1. INTRODUCTION

Extreme environments are considered to enclose a large variety of exceptional and yet unexplored microbial life (1). Such environments are represented by the High-Altitude Andean Lakes (HAAL), pristine ecosystems located at the Dry Central Andes region between 2000 and 6000 m above sea level, asl (2, 3). Predominant harsh conditions at the HAAL are strong UV irradiation, desertic weather and large temperature fluctuations during the day, alkalinity, hypersalinity (up to 30%), and volcanic settings together with a high concentration of arsenic on soils and in water (up to 200 ppm) as a consequence of geological foundation (2, 3). Yet, an outstanding microbial diversity has developed there, and almost 500 strains of prokaryotes (archaea, cyanobacteria and eubacteria) and lower eukaryotes (fungi and yeast) were isolated from bacterioplankton, benthos, microbial mats and soils surrounding the lakes (4-7). Even microbial mats ordered in multi-layered flat mats and stubby pillars called stromatolites were found widespread at the HAAL; these stromatolites are the first ones described at such extreme environments and high altitudes (8).

The extremophilic *Acinetobacter* sp. Ver3 from HAAL was previously described as an exceptionally UV-resistant strain (4, 7). This strain was isolated from Lake Verde (4,400 m asl), a hypersaline lake in the HAAL. Recently, we could provide evidence that this interesting UV-resistance phenotype is due in part to efficient photorepair capability (9), coupled to highly efficient antioxidant enzyme activities in response to UV-B stress (6).

Photorepair (PR) of living cells is also called photoreactivation, indicating that after a detrimental effect of UV irradiation in a cell population, the cells “revive” upon white light irradiation for an adequate time before plating (10). In this process, photo-activated enzymes, called “photolyases”, are the main protagonists. These molecules are phylogenetically well conserved monomeric proteins of 53 - 66 kDa that contain flavin adenine dinucleotide (FAD) as cofactor and antenna pigments such as 5,10-deazaflavin or methenyltetrahydrofolate (MTHF) derivatives (10). Recently, we reported the existence of a full-length putative

photolyase-coding gene in extremophilic *Acinetobacter* sp. Ver3, which displays moderate sequence similarity to the class I CPD-photolyase of *E. coli* (41%) (9).

These former findings called for a more detailed, molecular investigation. We thus present here a functional characterisation, which demonstrates that the photolyase from *Acinetobacter* sp. Ver3 is indeed responsible for the efficient photorepairing ability of this strain. All studies were performed in parallel with the ortholog enzyme from *E. coli*, allowing for a direct comparison of both recombinant proteins.

2. MATERIALS AND METHODS

2.1. Bacteria and culturing techniques

UV-resistant strain *Acinetobacter* sp. Ver3 was previously isolated from Lake Verde (4,400 m asl) at the Andean Puna (4, 7) and currently maintained in the culture collection of Laboratory of Microbial Research on Andean Lakes (National System of Biological Data). *Escherichia coli* BL21 was used as the recipient strain for the cloning experiments but also as a sensitive control in the UV-resistance assays. For comparative assays, BL21 containg a pET28 vector encoding the EcPhr (class I CPD-photolyase from *E. coli*), and the following *E. coli* strains were used (see also Table 1): KY1225, KY1056, KY1225 pREP4 and KY1225 pREP4 pQE60-EcPhr (11). For preculture and UV resistance assays, all strains were grown in LB media or on LB-agar plates (15.0 g/L). For overexpression, cells were grown on TBY broth. Depending on the resistance, cultures were supplemented with antibiotics at the following final concentrations: kanamycin (Kan), 50 µg/mL; tetracycline (Tc), 20 µg/mL; chloramphenicol (Cm), 30 µg/mL and ampicillin (Amp), 100 µg/mL. For longer periods, plasmids were maintained in glycerol batches of *E. coli* XL1 cells at -80 °C.

2.2. Cloning and expression of *Acinetobacter* sp. Ver3 CPD-photolyase

The CPD-photolyase of *Acinetobacter* sp. Ver3 (hereafter, Ver3Phr) was PCR-amplified from genomic DNA (60"/95 °C, 60"/55 °C, 90"/72°C, 35 cycles; primer pairs: V3_PL_pEt52for: 5′CAG GGA CCC GGT ATG AAT CTC ATT GGG TTT AG and V3_PL_pET52rev: 5′GGC ACC AGA GCG TTG GCT GAT TTG AAA GCA G). Primers were designed to introduce a 12 bp 5′ extension into the sense and a 14 bp 5′ extension into the antisense to generate the vector-specific complementary ends for ligation-independent cloning into the antisense primers (underlined). The PCR product was cloned into a linearised pET52 3C/LIC vector using the 3C/LIC cloning kit (Novagen) according to manufacturer's protocol. The plasmid carrying the 1411 bp insert was designated pET52-Ver3Phr. In all cases, cloning products were sequenced in order to confirm their identity. The recombinant protein was expressed in transformed *E. coli* BL21 (DE3) RIL (Stratagene, USA) cells carrying the pET52-Ver3Phr vector. Cultures were grown at 37 °C to an optical density of 0.5 measured at 600 nm, at which expression of the recombinant protein was induced by the addition of isopropyl-beta-D-thiogalactopyranoside (IPTG, 1.0 mM final concentration). After 4–5 h, cells were harvested, disrupted in liquid nitrogen using an ULTRA TURRAX (Milian, Geneva, Switzerland), and the Ver3Phr protein was purified from the soluble fraction by affinity chromatography on a Ni^{2+}-IDA resin. Washing and elution were performed as recently described (12). Imidazole was removed by passing the protein extracts in several steps through AMICON ULTRA-15 centrifugal filters units (30 kDa). For storage and spectroscopy measurements, purified proteins were resuspended in 50 mM Tris-HCl, 50 mM NaCl, 20% glycerol, 1 mM EDTA, 1 mM DTT. Similar procedure was performed for obtaining the pure Class I CPD-photolyase from *E. coli*, which was used as reference. In this case, the BL21 cell carrying a pET28-EcPhr vector (Table 1) was employed. The resulting protein fractions were analysed by 12% SDS polyacrylamide gel electrophoresis and Western immunoblotting was performed using a His-specific antibody and the XCell II™ Blot Module (Life Technologies, Carlsbad, CA, USA) following the manufacturer recomendations. The

gels were visualized using a Gel Doc™ XR+ with Image Lab™ software (BioRad). Relative expression of the overexpressed protein was estimated by image processing using the freeware ImageJ (http://rsb.info.nih.gov/ij/). The original images were transformed to an 8-bit-picture, colors were inverted and background was substracted. A histogram was obtained using relative density of each band in the gel. The obtained values were used for representing band density in Figure S1 (Supplementary Material).

Gel plugs of the desired protein were excised manually, purified and trypsin-digested enzymatically as previously described (13). The resulting peptides were analysed by mass spectrometry (MALDI-TOF MS, Applied Biosystems Voyager-DE PRO, Foster City, USA) and the sequence of obtained peptides was matched with the predicted digested protein sequence using the Interactive FindPept analysis tool (http://web.expasy.org/tools/findpept/findpept-doc.html) (Supplementary Material S2).

For complementation assays the CPD-photolyase Ver3Phr was PCR-amplified from genomic DNA under similar conditions as before but using different primer set: PL1F-BamH1: 5´GC GGA TCC ATG AAT CTC ATT TGG TTT CGT (forward) and PL1R-BglII: 5´GA AGA TCT GGC TGA TTT GAA AGC AGC TAA (backward). Primers were designed to introduce a BamHI restriction site into the sense and a BglII restriction site into the anti-sense (underlined) for directional cloning the PCR product into a linearized pQE60 vector following standard methods. The plasmid carrying the 1411 bp insert sequence was designated pQE60-Ver3Phr. In all cases, cloning products were sequenced in order to confirm their identity. This plasmid was used to complement the photolyase deficient, UV sensitive KY1225 pREP4 strain (hereafter KY1225 pREP4 pQE60-Ver3Phr, Table 1).

2.3. Sequence analyses

The sequence of the CPD-photolyase protein-coding gene from *Acinetobacter* sp. Ver3 has been deposited in GenBank (Acc. HQ443199). All sequences of photolyase-related

proteins were retrieved from public databases via the National Center for Biotechnology Information web site (www.ncbi.nlm.nih.gov). Multiple sequence alignments were carried out using ClustalW2 (http://www.ebi.ac.uk/Tools/clustalw2/index.html). The phylogenetic tree was constructed with PhyML3.0 (14) using the Jones-Taylor-Thornton rate matrix (15) with 100 bootstrap replicates. A consensus of the 100 resulting trees was selected for further processing and visualisation using iTOL (16).

2.4. Characterization of Ver3Phr by UV/Vis spectroscopy

UV-vis absorbance spectra of recombinant proteins were measured under temperature control in a Shimadzu UV-2401PC spectrophotometer at 20 °C. Steady-state fluorescence measurements were carried out with a Perkin-Elmer LS50 luminescence spectrometer also at 20 °C.

The identity and stoichiometry of the chromophores were determined by spectroscopic analysis of purified proteins (17). The concentration of the apoenzyme was determined from the absorbance value at 280 nm using the theoretical extinction coefficient (ε_{280}: 104,070 M^{-1} cm^{-1})(17). To determine the FAD concentration, the holoprotein was denatured at 95 ºC for 5 min in a buffer containing 50 mM Tris-HCl (pH 7.5), 50 mM NaCl, 5 mM EDTA, and 1 mM DTT (17). The denatured protein was removed by centrifugation before the absorption spectrum of the released material was recorded. Under these conditions, MTHF is converted to 10-formyl tetrahydrofolate which does not absorb >300 nm and therefore does not interfere with flavin absorbance in the 400-500 nm range (18), now allowing determination of the FAD concentration from the 450 nm absorbance based on ε_{450} = 1.13 10^4 M^{-1} cm^{-1}). In addition, FAD, obtained as before, was quantified by fluorescence emission at 520 nm following excitation at 440 nm. In this case, the concentration of FAD was obtained by interpolation from a standard curve plotting fluorescence intensity versus known amounts of FAD.

Fresh standard solutions of MTHF or FAD in the same buffer used than for the enzymes were prepared immediately before each spectral run, considering in particular that MTHF is able to oxidate at neutral pH under long-term storage (19).

2.5. Determination of chromophores by HPLC

The protein-bound chromophores were released by heat denaturation under identical conditions as described above. After centrifugation, the supernatant was used for HPLC analysis. Each injection was repeated two times to follow statistical errors. A 1260 LC System (Agilent) was used, employing a 50 mm Zorbax SB C18-RP column (4.6 mm i.D.) and methanol / 10 mM TEAA (triethylammonium acetate) at pH 5.74 as solvents. A solvent gradient (t = 0, 85:15 A:B, t = 5 min, 70:30 A:B) was applied. Authentic FMN, FAD, and riboflavin (Sigma-Aldrich, St. Louis, MO) were taken as reference compounds. Besides, absorbance spectra of the eluted samples were recorded during the separation by a diode array detection system. Released chromophores were also subjected to steady-state fluorescence measurements.

2.6. Complementation assays and *in vivo* photoreactivation.

UV-B resistance and photoreactivation of recombinant strains expressing Ver3Phr were tested by a cell survival experiment (9). Selected strains were grown in LB medium at 30 °C with shaking (200 rpm), and cells were harvested in the mid-exponential phase by centrifugation (8,000 rpm, 30 min, 4 ºC). The pellets were washed twice in 0.9 % NaCl and then resuspended in the same solution, containing the appropriate antibiotics corresponding to each recombinant clone. A portion of each cell suspension (OD_{600}: 0.6; 20 mL) was exposed to UV-B irradiation at 30 cm distance using the light of a UVB lamp for 5 min (1.2 kJ m^{-2}) (Vilbert Lourmat VL-4; λ_{max} at 312 nm with average intensity of 0.387 mW cm^{-2}) with shaking (50 rpm) at 20 ºC. Controls were incubated in the dark under otherwise identical

conditions. After UV, 100 µL-aliquots were removed from the tubes, subjected to a dilution series in 0.9 % NaCl (10^{-1} to 10^{-5}), and 100 µL-aliquots from each dilution were plated on agar plates. This treatment allows us to assess the dark-repair ability of the treated cells immediately following the exposure (indicated as UV5 herein). Single colonies able to grow for each dilution were determined after 24 h of incubation at 37 ºC in the dark. For reference, it is worth to mention that non-exposed controls of all strain cultures plated at initial time (T0) reached a mean value of 1.5 x10^6 UFC/ml. Some treatments produce nule growth on agar plates (no UFC) even at the lowest dilution (10^{-1}) and this was computed in the graphic as zero values. The detection limit was 1 x10^2 UFC/ml. Microbial growth was recorded as percentage of the non-exposed cells.

UV-B exposed cell suspensions were subjected to photo repair (PR herein) by incubation under photo-active radiation (PAR) during 120 min (18 W m^2) using OSRAM L18 W/77 lamps with continuous shaking (50 rpm) at 15 ºC. A parallel control was incubated in the dark under the same conditions (DR herein). After each treatment, 100 µL-aliquots were removed from the tubes, subjected to a dilution series (10^{-1} to 10^{-5}), and plated on agar plates as explained before. The cells were incubated for 24 h at 37 ºC in the dark. Microbial growth was recorded as percentage of the non-exposed cells.

Manipulation of all cultures after UV, dark or PAR treatments were made in close room under yellow light (ROSCO supergel medium yellow ROS-010R, ROSCO LABORATORIES, USA) in order to prevent the photoreactivation of cells during dilution and inoculation of samples.

2.7. DNA purification and bipyrimidine photoproduct measurements by HPLC-ESI-MS/MS.

Extent of DNA damage after UV-treatment and photoreactivation of mutant, wild type and recombinant strains were determined to directly assess the activity of the overexpressed

proteins. For DNA preparation, cell suspensions (10 mL) from different treatments- UV-B exposed for 5 min (UV5), photorepaired cells (PR), dark-repaired cells (DR) and non-exposed controls at initial time (T0), 5 min (T5) and 125 min (T125) of each strain- were collected by centrifugation at 3,000 g for 10 min at 4 ºC and washed twice with distilled water. Extraction of total genomic DNA was performed in duplicate by using a commercially available genomic DNA kit (DNeasy Blood & Tissue Kit, Qiagen, Hilden, Germany) following the manufacter´s recommendations.

Several types of photoproducts including cis-syn CPDs, thymine-thymine (TT), thymine-cytosine (TC), cytosine-thymine (CT), and cytosine-cytosine (CC) sites, and pyrimidine-(6-4) pyrimidone photoproducts (6-4PPs) at thymine-thymine and thymine-cytosine sites were measured in total genomic DNA from each treatment using previously optimised procedures (20, 21). Briefly, extracted DNA solubilized in an aqueous solution of 0.1 mM deferroxiamine mesylate was enzymatically hydrolysed by incubation with nuclease P1, DNase II and phosphodiesterase II (2 h, 37 °C, pH 6), followed by a second digestion step involving phosphodiesterase I and alkaline phosphatase (2 h, 37 °C, pH 8). The digested samples were injected onto an HPLC system consisting in a Agilent series 1100 system equipped with a Uptisphere ODB reverse phase column (2 x 250 mm ID, particle size 5 µm; Interchim, Montluçon, France) using as mobile phase a gradient of acetonitrile in a 2 mM aqueous solution of TEAA as the mobile phase. For determinating the amount of analysed DNA, quantification of normal nucleosides was performed with a UV detector (260 nm). The HPLC flow was then directed toward an API 3000 electrospray triple quadrupole mass spectrometer operating in the negative ionisation mode. External calibration was achieved using reference compounds and the corresponding calibration curves. Results were expressed as number of photoproducts per 10^6 DNA bases.

Standards for the HPLC-ESI-MS/MS were synthesized according to previously published procedure (22). In brief, dinucleoside monophosphates were prepared by triester

synthesis. CPDs were obtained using acetophenone and UVA by photosensitized triplet energy transfer. 6-4PPs were prepared by UVC photolysis. Additional UVA irradiation of the latter compounds yielded the Dewar valence isomers. All photoproducts were purified by HPLC.

2.8. Statistical analyses.

Statistical analyses were conducted using the Microcal™ Origin Working Model Version 6.0. Paired *t*-test and ONE WAY ANOVA variance analysis were done with a probability level of $p<0.05$. All experiments were carried out in duplicates.

3. RESULTS AND DISCUSSION

3.1. Comparison of the deduced Ver3Phr protein sequence with other photolyases

A multiple sequence alignment of the Ver3Phr sequence with other known phr sequences in the GenBank database indicated that the Ver3Phr sequence was most similar to that of class I CPD photolyases (data not shown). Thus, we performed phylogenetic studies to clearly probe this affiliation (Fig. 1A), including representatives of the major groups of branches within the cryptochrome-photolyase family (Supplementary material, S3): CPD photolyases class I to III, Cry-DASH, which are single-strand specific photolyases, in most cases displaying an additional transcriptional regulatory function(23), (6-4) photolyases together with animal Cry, plant Cry and a new class, named CryPro (24). As expected, Ver3Phr branched together with typical CPD Class I photolyases, which includes the most extensively studied *E. coli* photolyase (for a review, see ref (25)). The closest neighbor, however, was the CPD-photolyase from *Pseudomonas aeruginosa*, which is also a member of the Gamma Proteobacteria class. This opportunistic human and plant pathogen has been studied extensively for its photoreactivation ability. Although the phr sequence of *Pseudomonas aeruginosa* PAO1 was identified from the genome sequence, cloned, and

shown to complement a known phr mutation following expression in *Escherichia coli* SY2 (26), accurate functional analyses of this Gamma proteobacterium photolyase itself or any other from this taxonomical group have not been reported till present.

The deduced amino acid sequence of Ver3Phr showed an overall low sequence similarity (41 %) to the ortholog protein from *E. coli* (Fig. 1B), although the secondary structure prediction and signatures typical and essential for photolyases were clearly identified. Inspection of the sequence in comparison with canonical CPD-photolyases reveals the canonical tryptophan triade (asterisks), fully conserved at identical positions in the sequence. Also those residues in direct interaction with the FAD chromophore (diamonds), identified from the *E. coli* enzyme crystal structure, are fully conserved except for position 236 (arginine in the *E. coli* enzyme vs. glutamine-238 in Ver3Phr). Similarly, those amino acids, interacting with the MTHF cofactor (arrowheads), are identical except for C292 (*E. coli*), which is changed into serine in Ver3Phr (S297). A model-building approach of Ver3Phr tridimensional structure with that of the ortholog protein from *E. coli* was performed previously (9). The structure revealed a proximal alpha-beta domain and a distal helical domain that binds the FAD in full accordance to the structure of the *E. coli* photolyase (27).

3.2. Overexpression of the photolyase gene from *Acinetobacter* sp. Ver3 and spectroscopical characterization

The gene encoding Ver3Phr was successfully cloned and overexpressed. The protein could be purified to homogeneity, using affinity chromatography (Ni-NTA) (Fig. 2A), followed by gel filtration (Fig. 2B). Electrophoresis shows an apparent molecular mass of ca. 60 kDa, which is in accord with the predicted mass of 54.7 kDa for His tag Ver3Phr. Western blot (Fig. 2C) and mass spectrometry (MALDI-TOF-MS) analysis of the gel-extracted, trypsin digested 60-kDa band confirmed the identity of this protein (Supplementary material, S2).

All experiments dedicated to the functional analysis of Ver3Phr were performed in parallel also with photolyase of *E. coli* including identical procedures for purification. Nevertheless, purified photolyases were obtained in somewhat different yields (for Ver3Phr was ca. four-fold lower than for EcPhr), chromophore loading (100% loading of FAD for EcPhr and 80% loading for Ver3Phr) and dissimilar redox states (Fig. 3A). Note that expression of proteins in the recombinant cells was evaluated by a quantitative Western analysis (Supplementary material, Fig. S1), showing even higher expression of the Ver3Phr in the pET vectors, compared to EcPhr, indicating that low yields obtained in the purification process are rather due to the instability of the protein.

The absorption spectrum of EcPhr shows the characteristic absorption bands of the oxidised form of FAD (FADox) around 380 and 450 nm (Fig. 3A), in agreement with published results (25). However, the absorption band ratio between 380 nm and 450 nm is larger than for isolated FAD chromophore in solution, as consequence of light scatering effect in the protein samples and/or the presence of other chromophore. The contribution of MTHF to the 380 nm peak in *E. coli* photolyase should be much higher that from oxidized FAD although in the UV spectra obtained is not possible to distinguish this contribution, most probably a consequence of the low protein yield and/or partial destruction of MTHF during purification.

The UV-vis spectrum of Ver3Phr showed a different pattern; instead, a blue-shifted absorption band with a small peak around 420 nm was observed, in accordance with the absorbance spectrum of a partially or fully reduced flavin (28). Even when the protein was eluted and kept overnight in a non-reducing buffer (i.e. without DTT), the spectrum of Ver3Phr did not change to a more clearly observable oxidised state of FAD (data not shown). With the exception of *Saccharomyces cerevisiae* photolyase, the flavin cofactors of all photolyases characterised to date become oxidised to the FADH• blue-neutral radical or to FADox during purification (25). Nevertheless, traces of FADox cannot be excluded as co-

factor into the protein, as both, the fluorescence excitation and emission spectra, (Fig. 3B) of Ver3Phr were very similar to those observed for oxidised flavins in buffer solutions (29). The ratio of the fluorescence integrated area divided by the absorption of the solution at 440 nm of each protein sample with that for FAD in the buffer solution was ≈ 4.6 and 0.3 for EcPhr and Ver3Phr, respectively. Therefore, an enhanced emission of FADox is observed for EcPhr, probably due to a larger molecular rigidity imposed by the protein backbone. Instead, for Ver3Phr the lower fluorescence intensity ($\Phi_F \leq 10^{-2}$) reflects the lesser amount of the oxidized form of FAD in this enzyme. Therefore, despite of the lower emission quantum yield of Ver3Phr both the emission and excitation fluorescence spectra show the typical fluorescence fingerprint of FADox, comfirming its presence of traces of the oxidized cofactor in this enzyme, as suggested before. In fact, as it is shown in Fig. 3B, the FADox fluorescence emission of Ver3Phr is slightly blue shifted at 518 nm, as compared with the maximum observed at 524 nm for EcPhr and at 526 nm for the flavin in buffer solution. Furthermore, VerPhr showed a smaller Stokes-shift than those observed for EcPhr and FAD alone, respectively. These spectral behaviors indicate that the isoalloxazine ring in Ver3Phr senses a less polar binding pocket than EcPhr, probably related to the Arg/Gln change mentioned in the former section.

Furthermore, the presence of FAD-chromophore in Ver3Phr was also confirmed by HPLC analysis after protein heat-denaturation (data not shown). In this procedure FAD was also detected in its oxidised state, as recorded by fluorescence spectroscopy (see above).

The presence of MTHF as antenna pigment in native Ver3Phr was established also by spectroscopy. Under buffer conditions used in this work, the absorption maximum of MTHF is about 55 nm blue shifted as compared with that observed in ultra-pure water (e.g. 357 nm), (see Supplementary material Fig. S4). This effect can be associated with the complex composition of the working buffer (see section 2.6). By comparing the fluorescence emission with selective excitation at 330 nm in the MTHF absorption band, with that of native EcPhr

and a standard MTHF solution, the MTHF-like emission maximum in VerPhr (λ_{max}^{em} = 411 nm) and EcPhr (λ_{max}^{em} = 422 nm) is red-shifted compared with that at 400 nm for the antenna pigment in buffer (Fig. 3C). This behaviour is expected for MTHF bound to enzymes due to specific interactions in addition to the effects of local rigitidity and lower polarity that may be imposed on the antenna pigment by the enzyme-binding site (19). However, for both enzymes, excitation at 330 nm also produces a weak FADox emission around 510 nm, indicating poor energy-transfer efficiency between MTHF and FAD.

3.3. Photorepairing activity of Ver3Phr in *E. coli* host cells

A functional complementation analysis of the Phr gene of *Acinetobacter* sp. Ver3 using photoreactivation-deficient *E. coli* KY1225 cells as hosts (11) was performed in order to clarify whether Ver3Phr demonstrates significant photolyase activity *in vivo*. Thus, UV-B resistance pattern and photoreactivation ability of *E. coli* KY1225 host cells was compared with the transformant carrying the VerPhr (KY1225 pREP4 pQE60-Ver3Phr) and the one carrying the phr gene of *E. coli* (KY1225 pREP4 pQE60-EcPhr) together with its wild-type KY1056 (Fig. 4-6). Two methods were used for this purpose: i) to directly assess the level of DNA damage after each treatment, CPDs were measured by HPLC-ESI-MS/MS in genomic DNA extracted from aliquotes of cultures at different times: immediately after UV treatment (UV5), or after the UV-treated cells were left for recovery in light (PR) or dark (DR) for 120 min; ii) duplicate aliquots were taken from these three treatments, plated and incubated in the dark for 24 h in nutrient media. Note that even when treatments were identical and aliquots were taken in duplicates at the same time, the first analytical technique measured the genuine damage in cells immediately after each treatment while the second one indicated which fraction of those aliquots were able to recover and duplicate in the dark during the incubation period (24 h) in spite of the photodamage.

Our results demonstrate that the UV dose used was effective for producing a significant damage to genomic DNA (Figs. 4, 5) and affecting cell viability (Fig. 6) of tested strains: wild-type KY1056 and its mutant strain KY1225 alone or overexpressing Ver3Phr or EcPhr. Non-exposed control cultures of all four strains displayed mean values of 11 to 21 CPDs per 10^6 bases (data not shown) while UV exposure increased this value up to twenty-fold (Fig. 4). Recipient mutant strain KY1225 and its wild-type KY1056 were by far the most affected ones, depicting absolute mean values of photodamage as high as 219 and 236 CPDs per 10^6 bases, respectively (Fig. 4). In all cases, dimeric pyrimidine photoproducts were not equally generated; TT-CPDs were the most abundant photoproducts, followed by TC>CT>CC, confirming TT as preferred UV-targets in *E. coli* (30). Pyrimidine-(6-4) pyrimidone photoproducts (6-4PPs) were also detected in DNA extracted from the different strains but in much lower proportion compared to CPDs: only 3 to 5 6-4PPs per 10^6 bases after UV5 treatments compared with 0 to 2 6-4PPs per 10^6 bases in the non-exposed controls (data not shown), and thus, the analysis of results that follows will be based only on CPDs measurements.

DNA damage after the UV5 treatment was 58% and 90% lower in the KY1225 strains overexpressing Ver3Phr and EcPhr, respectively, compared with the KY1225 alone (Fig. 4). This premature depletion of CPDs during the UV exposure in both recombinant strains -much highlighted in EcPhr- in absence of the theoretically activating light, i.e., wavelengths within the 370-500 nm range (UV Spectra of Vilbert Lourmat VL-4, Manufacturer´s brochure) can only be attributed to the overexpressed photolyases and explained by three alternative hypothesis: i) an effective function of the photorepairing early during the UV-B exposure (300-360 nm), likely because MTHF absorb photons in the range 300-500 nm or due to the absorbance of photons by the fully reduced FAD (350 nm); ii) a protective action of the enzyme molecules produced by a non-specific binding to undamaged DNA that shields the UV-B radiation and precludes the formation of bipyrimidine photoproducts in the

corresponding strand region. Several authors indicate that photolyase is able to bind non-specifically to undamaged DNA (31, 32), especially when present at high concentrations (33); iii) enhancement of nucleotide excision repair (NER) efficiency by photolyases. Nonphotoreactivation function of photolyases was a common observation in early works (34-36) although not quite studied thereafter (25, 37). The fact that photolyases are highly expressed in animal tissues from internal organs where direct UV-exposure is not possible favours the idea that photolyases play an additional role in repair (38). Actually, without photoreactivating light, photolyases bind pyrimidine dimer photoproducs and stimulate the removal of UV damage *in vivo* (11, 34, 36) and *in vitro* (35, 36).

The analysis of depletion percentage for different bipyrimidine photoproduct types revealed that CC CPDs are almost scarcely depleted in both recombinant strains compared to KY1225 (Fig. 4). Myles et al. (1987) (39) found that C-containing CPDs, in particular CC-dimers, were not efficiently repaired by photolyase and they could also demonstrate that stimulation of NER enzymes by photolyases is poorer for the same dimeric photoproducts, this being further proof that the stimulation was due to direct interaction between the photolyase and the excision nuclease when bound to DNA (more discussion about this point is given below). In addition, these results confirmed earlier observations (40) that the content and base sequence within the dimeric photoproduct influence repair and showed that preference is due, at least in part, to differences in binding affinity.

The much larger percentage of repairing for EcPhr-carrying strains is not likely related to a higher concentration of photolyases in the cell as the Western blot indicated that the expression of photolyases was rather similar for both recombinant strains (Supplementary material, Fig. S1) while loading with the chromophore was indeed smaller in Ver3Phr and may account for a smaller fraction of active enzymes.

In accordance with the level of DNA damage, UV-exposed cells (UV5, without photoreactivation) were not able to proliferate when plated onto nutrient media, with the only

exception of a minor fraction (28%) of the recombinant strains carrying the EcPhr gene (Fig. 6). It seems that photodamage higher than 90 CPDs per 10^6 bases is incompatible with proliferation of *E. coli* cells in contrast with the case of HAAL *Acinetobacter* sp. strains (including Ver3) that can withstand and proliferate well after levels of photodamage as high as 900 CPDs per 10^6 bases (9).

After UV-exposure, cell suspensions were left under PAR (w/photoreactivation) for 120 min in the same saline solution with shaking. As expected, the double mutant, KY1225 (Phr^- and RecA), was not able to diminish significantly the frequency of photoproducts under light (Fig. 5) as the enzyme responsible for this ability was knocked-out (11), and, consequently, no recovery was seen when cells were plated in nutrient media (Fig. 6). In turn, KY1056, constitutively expressing its original photolyase was able to diminish considerably the levels of CPDs (75%, Fig. 5); the minor photodamage allows this strain to recover its cell population to 70% after PR (Fig. 6).

Functional complementation was clear for both recombinant strains expressing EcPhr or Ver3Phr. Levels of CPDs decreased under PAR (Fig. 5), strongly in Ver3Phr (90%) and less pronounced for EcPhr (22%) when compared with CPDs measured for the corresponding UV5 treatments. Consequently, both transformants were able to almost fully recover when plated in agar media, yielding 85 and 78 % of the initial value for Ver3Phr and EcPhr, respectively (Fig. 6).

The parallel controls left in the dark during 120 min before plating gave striking results. KY1225 and KY1056 (both lacking recombinant repair but not nucleotide excision repair, NER) depicted similar low levels of repair under these conditions: only 8-6% reduction of the levels of CPDs was noted compared to the corresponding UV5 treatments (Fig. 5). Accordingly, no recovery was observed when aliquots of these cells were plated in agar media (Fig. 6). For recombinant strains, dark repair was significantly higher: depletion of 15% for Ver3Phr and of 23% for EcPhr (Fig. 5), which allows the treated cells to grow well

when plated in agar media (Fig. 6). This minor but significant activity of overexpressed photolyases in the dark may be explained by the known fact that photolyases stimulate NER in several prokaryotes and eukaryotes tested (34-36, 41, 42) (26). Excision repair is a light-independent but ATP-dependent multi-subunit general repair system that eliminates virtually all types of DNA lesions by making single-stranded DNA scissions for bracketing the lesion and removing the damage (43).

Altogether, these results indicate that the protein encoded by the Phr gene of *Acinetobacter* sp. Ver3 has a strong photoreactivation activity while its contribution to enhance repair mechanisms in the dark is poorer compared to its *E. coli* homologue. A similar outcome was described for the complementation of Phr^- mutants of *E. coli* with yeast photolyase (PHR1): the photoreactivating function of the yeast PHR1 gene was succesfully complemented in the heterologous host, but the stimulation of NER was not possible (36). Nevertheless, PHR1 complementing a Phr^- mutant of the same yeast was able to stimulate both mechanisms. These results were explained by the formation of a ternary complex among the dimer, the photolyase and the ABC nuclease excision complex that incises the damaged strand at some distance from the pyrimidine dimer photolesion. This means that the interaction with the dimeric pyrimidine photoproduct and the photolyase of yeast precludes the incision of the ABC nuclease complex of *E. coli* but not the incision of the similar nuclease complex in yeast (36). The inhibition of the bacterial excision nuclease by yeast photolyase likely reflects the necessity of coevolution of photolyases and the NER complex for a function in combination (44) (36). Current work is being conducted to express Ver3Phr gene in *E. coli* and Ver3 double mutant strains ($uvrA^-$/$uvrB^-$/$uvrC^-$ and phr^-) in order to reveal if this phenomenon is due to a structural and/or functional difference between the photolyases or whether it is a matter of differential expression in a heterologous host.

4. CONCLUDING REMARKS

In this work, we have successfully cloned and overexpressed in a heterologous host a photolyase gene from a UV-resistant strain originally isolated from the HAAL. To our knowledge this is the first report of a functional photolyase in a bacterial extremophile and the first detailed characterisation of a photolyase belonging to this genus.

The amino acid sequences of *E. coli* photolyase and the Ver3 photolyase exhibit moderate 41% identity although comparison with canonical CPD-photolyases reveals the typical tryptophan triade fully conserved at identical positions in the sequence. Likewise, those residues in direct interaction with the FAD chromophore and the MTHF cofactor are fully conserved except for position 236 (arginine in the *E. coli* enzyme vs. glutamine-238 in Ver3Phr) and C292 (*E. coli*), which is changed into serine in Ver3Phr (S297), respectively. The spectroscopical measurements confirmed MTHF and FAD as antenna and cofactor, respectively, and indicated that the Ver3Phr protein was obtained mainly in its fully reduced form.

Functional complementation of Ver3Phr in Phr$^-$-RecA strains was assessed by two methods; the first took in consideration the fraction of cells able to proliferate in nutrient media after the treatment which, otherwise, was the most commonly used indirect method, to assess photorepair efficiency in all related or similar works (11, 34, 35, 45). Additionaly, we have clearly demonstrated that the observed survival percentage was indeed due to an augmentation or depletion of the frequency of bipyrimidine photoproducts in the DNA, directly and accurately measured by a powerful and sensitive analytical, technique such as HPLC-ESI-MS/MS in the multiple reaction monitoring mode. Thus, the results clearly point out to strong photoreactivation ability *in vivo* of Ver3 photolyase while its nonphotoreactivation function, most probably related with the stimulation of NER pathway, was not as manifest as for EcPhr. Whether this is a question of the the system used, i.e. an exogenous photolyase (*Acinetobacter*) incorporated in a different cell line (*E. coli*), or a

fundamental different behaviour of a novel enzyme from an exotic environment (HAAL) will need further studies.

Finally, we would like to emphasise that these findings are of importance, as they constitute pioneer work on elucidating of molecular mechanisms supporting the outstanding UV resistance of a model extremophilic strain from the HAAL, considered one of the highest UV exposed ecosystems on Earth (8, 46). Further works are in process to assess *in vitro* repair of Ver3Phr compared to *E. coli* and other well-known photolyases from non-extremophiles in order to test if the extreme UV-irradiated origin of the strain indeed supported a more efficient molecular system for removal of DNA photolesions.

ACKNOWLEDGEMENTS

The authors acknowledge the generous financial support by the PICT 2006 01090 Project (FONCyT, Argentina), the Proalar Agreement (MINCYT-DAAD) DA/09/05 and MPI for Chemical Energy Conversion, Germany. A Marie Curie FP7-People-2010-IIF EXTREMOPHIL (273831) in Germany and its return phase in Argentina (PIIFR-GA-2010-910831-EXTREMOPHIL) supports research work of V.H.A. M.E.F., C.D.B and V.H.A. are researchers from the National Research Council (CONICET) in Argentina.

We are greatly indebted to Prof. A. Batschauer and Dr. R. Pokorny, Univ. Marburg, Germany, for providing the *E. coli* strains and plasmids used in this work, and for their helpful discussion.

REFERENCES

1. M. J. Seufferheld, H. M. Alvarez and M. E. Farias, Role of polyphosphates in microbial adaptation to extreme environments. *Appl. Environ. Microbiol.*, 2008, **74,** 5867-74.
2. V. H. Albarracín, Dib, J. R., Ordoñez, O. F., Farias, M. E., A Harsh Life to Indigenous Proteobacteria at the Andean Mountains: Microbial Diversity and Resistance Mechanisms Towards Extreme Conditions. In *"Proteobacteria: Phylogeny, Metabolic Diversity and Ecological Effects"*. (Edited by M. L. Sezenna), 2011, pp. 91-131. Nova Science Publishers.
3. V. H. Albarracín, D. Kurth, O. F. Ordoñez, C. Belfiore, E. Luccini, G. M. Salum, R. D. Piacentini, M. E. Farias, High-Altitude Andean Lakes. A remote reservoir of micro-biodiversity under extreme enviromental conditions. *Astrobiology*, 2013, AST-2013-1109, in revision.
4. M. R. Flores, O. F. Ordonez, M. J. Maldonado and M. E. Farias, Isolation of UV-B resistant bacteria from two high altitude Andean lakes (4,400 m) with saline and non saline conditions. *J. Gen. Appl. Microbiol.*, 2009, **55,** 447-458.
5. J. Dib, J. Motok, V. F. Zenoff, O. Ordonez and M. E. Farias, Occurrence of resistance to antibiotics, UV-B, and arsenic in bacteria isolated from extreme environments in high-altitude (Above 4400 m) andean wetlands. *Curr. Microbiol.*, 2008, **56,** 510-517.
6. C. Di Capua, A. Bortolotti, M. E. Farias and N. Cortez, UV-resistant *Acinetobacter* sp isolates from Andean wetlands display high catalase activity. *FEMS Microbiol. Lett.*, 2011, **317,** 181-189.
7. O. F. Ordonez, M. R. Flores, J. R. Dib, A. Paz and M. E. Farias, Extremophile culture collection from Andean lakes: extreme pristine environments that host a wide diversity of microorganisms with tolerance to UV radiation. *Microbial Ecology,* 2009, **58,** 461-73.
8. M. E. Farias, N. Rascovan, D. M. Toneatti, V. H. Albarracin, M. R. Flores, D. G. Poire, M. M. Collavino, O. M. Aguilar, M. P. Vazquez and L. Polerecky, The discovery of stromatolites developing at 3,570 m above sea level in a High-Altitude volcanic Lake Socompa, Argentinean Andes. *Plos One*, 2013, **8**.
9. V. H. Albarracin, G. P. Pathak, T. Douki, J. Cadet, C. D. Borsarelli, W. Gartner and M. E. Farias, Extremophilic *Acinetobacter* Strains from High-Altitude Lakes in Argentinean Puna: Remarkable UV-B resistance and efficient DNA damage repair. *Orig. Life Evol. Biosph.*, 2012, **42,** 201-221.
10. S. Weber, Light-driven enzymatic catalysis of DNA repair: a review of recent biophysical studies on photolyase. *Biochimica et Biophysica Acta*, 2005, **1707,** 1-23.
11. S. Akasaka and K. Yamamoto, Construction of *Escherichia coli* K12 PHR Deletion and insertion mutants by gene replacement. *Mutation Research*, 1991, **254,** 27-35.
12. G. P. Pathak, A. Ehrenreich, A. Losi, W. R. Streit and W. Gartner, Novel blue light-sensitive proteins from a metagenomic approach. *Environmental Microbiology,* 2009, **11,** 2388-99.
13. O. Jahn, D. Hesse, M. Reinelt and H. D. Kratzin, Technical innovations for the automated identification of gel-separated proteins by MALDI-TOF mass spectrometry. *Analytical and Bioanalytical Chemistry*, 2006, **386,** 92-103.
14. S. Guindon and O. Gascuel, A simple, fast, and accurate algorithm to estimate large phylogenies by maximum likelihood. *Syst. Biol.*, 2003, **52,** 696-704.
15. D. T. Jones, W. R. Taylor and J. M. Thornton The rapid generation of mutation data matrices from protein sequences. *Comput. Appl. Biosci.,* 1992, **8,** 275–282.
16. I. Letunic, R. R. Copley, B. Pils, S. Pinkert, J. Schultz and P. Bork, SMART 5: domains in the context of genomes and networks. *Nucleic Acids Res.*, 2006, **34,** D257-D260.

17. N. Ozturk, Y.-T. Kao, C. P. Selby, I. H. Kavakli, C. L. Partch, D. Zhong and A. Sancar Purification and characterization of a type III photolyase from *Caulobacter crescentus*. *Biochemistry*, 2008, **47,** 10255-10261.
18. J. L. Johnson, S. Hammalvarez, G. Payne, G. B. Sancar, K. V. Rajagopalan and A. Sancar identification of the 2nd chromophor of *Escherichia coli* and yeast DNA photolyases as 5,10-Methenyltetrahydrofolate. *Proc. Natl. Acad. Sci. U. S. A.*, 1988, **85,** 2046-2050.
19. S. T. Kim, Heelis, P. F., Okamura, T., Hirata, Y., Mataga, N., and Sancar, A., Determination of rates and yields of interchromophore (folate----flavin) energy transfer and intermolecular (flavin----DNA) electron transfer in *Escherichia coli* photolyase by time-resolved fluorescence and absorption spectroscopy. *Biochemistry*, 1991, **30,** 11262-11270.
20. T. Douki, M. Court, S. Sauvaigo, F. Odin and J. Cadet, Formation of the main UV-induced thymine dimeric lesions within isolated and cellular DNA as measured by high performance liquid chromatography-tandem mass spectrometry. *J. Biol. Chem.*, 2000, **275,** 11678-11685.
21. S. Mouret, P. Bogdanowicz, M. J. Haure, N. Castex-Rizzi, J. Cadet, A. Favier and T. Douki, Assessment of the photoprotection properties of sunscreens by chromatographic measurement of DNA damage in skin explants. *Photochem. Photobiol.*, 2011, **87,** 109-116.
22. T. Douki and J. Cadet, Individual determination of the yield of the main UV-induced dimeric pyrimidine photoproducts in DNA suggests a high mutagenicity of CC photolesions. *Biochemistry*, 2001, **40,** 2495-2501.
23. C. P. Selby and A. Sancar, A cryptochrome/photolyase class of enzymes with single-stranded DNA-specific photolyase activity. *Proc. Natl. Acad. Sci. U. S. A.*, 2006, **103,** 17696-700.
24. Y. Geisselbrecht, S. Fruhwirth, C. Schroeder, A. J. Pierik, G. Klug and L. O. Essen CryB from *Rhodobacter sphaeroides*: a unique class of cryptochromes with new cofactors. *EMBO Reports*, 2012, **13,** 223-9.
25. A. Sancar, Structure and function of DNA photolyase and cryptochrome blue-light photoreceptors. *Chem. Rev.*, 2003, **103,** 2203-2237.
26. J. J. Kim and G. W. Sundin, Construction and analysis of photolyase mutants of *Pseudomonas aeruginosa* and *Pseudomonas syringae*: contribution of photoreactivation, nucleotide excision repair, and mutagenic DNA repair to cell survival and mutability following exposure to UV-B radiation. *Appl. Environ. Microbiol.*, 2001, **67,** 1405-11.
27. H. W. Park, S. T. Kim, A. Sancar and J. Deisenhofer, Crystal structure of *E. coli* photolyase at 2.3A resolution. *Biophysical Journal*, 1995, **68,** A324.
28. Y. T. Kao, Saxena, C., He, T. F., Guo, L. J., Wang, L. J., Sancar, A., and Zhong, D. P., Ultrafast dynamics of flavins in five redox states. *J. Am. Chem. Soc.,* 2008, **130,** 13132-13139.
29. L. Valle, F. E. M. Vieyra and C. D. Borsarelli, Hydrogen-bonding modulation of excited-state properties of flavins in a model of aqueous confined environment. *Photochem. Photobiol. Sci.*, 2012, **11,** 1051-1061.
30. D. Chandrasekhar and B. Van Houten, *In vivo* formation and repair of cyclobutane pyrimidine dimers and 6-4 photoproducts measured at the gene and nucleotide level in Escherichia coli. *Mutat. Res.-Fundam. Mol. Mech. Mutagen.*, 2000, **450,** 19-40.
31. G. B. Sancar, Enzymatic photoreactivation: 50 years and counting. *Mutat. Res.-Fundam. Mol. Mech. Mutagen.*, 2000, **451,** 25-37.

32. J. van Noort, K. O. van der Werf, B. G. de Grooth and J. Greve, Conformation of individual photolyase dna complexes studied by atomic force microscopy. *Biophysical Journal*, 1999, **76,** A386-A386.
33. M. C. DeRosa, A. Sancar and J. K. Barton, Electrically monitoring DNA repair by photolyase. *Proc. Natl. Acad. Sci. U. S. A.*, 2005, **102,** 10788-10792.
34. K. Yamamoto, M. Satake, H. Shinagawa and Y. Fujiwara, Amelioration of the Ultraviolet sensitivity of an *Escherichia coli* RECA mutant in the dark by photoreactivating enzyme. *Mol. Gen. Genet.*, 1983, **190,** 511-515.
35. A. Sancar, K. A. Franklin and G. B. Sancar, *Escherichia coli* DNA photolyase stimulates UVR-ABC excision nuclease *in vitro*. *Proc. Natl. Acad. Sci. U. S. A.*, 1984, **81,** 7397-7401.
36. G. B. Sancar and F. W. Smith, Interactions between yeast photolyase and nucleotide excision repair proteins in *Saccharomyces cerevisiae* and *Escherichia coli*. *Mol. Cell. Biol.*,1989, **9,** 4767-4776.
37. R. P. Sinha and D. P. Hader, UV-induced DNA damage and repair: a review. *Photochem. Photobiol. Sci.*, 2002, **1,** 225-236.
38. Z. Ozer, J. T. Reardon, D. S. Hsu, K. Malhotra and A. Sancar, The other function of DNA photolyase: Stimulation of excision repair of chemical damage to DNA. *Biochemistry*, 1995, **34,** 15886-15889.
39. G. M. Myles, B. Vanhouten and A. Sancar, Utilization of DNA photolyase, pyrimidine dimer endonucleases, and alkalihydrolysis in the analysis of aberrant ABC excinuclease incisions adjacent to UV-induced DNA photoproducts. *Nucleic Acids Res.*, 1987, **15,** 1227-1243.
40. W. L. Carrier and R. B. Setlow, Excision of Pyrimidine Dimers From Irradiated Deoxyribonucleic Acid in vitro. *Biochimica Et Biophysica Acta*, 1966, **129,** 318-&.
41. D. Vlcek, S. Podstavkova and E. Miadokova Interactions between photolyase and dark repair processes in *Chlamydomonas reinhardtii*. *Mutat. Res.-DNA Repair*, 1995, **336,** 251-256.
42. F. Thoma, Light and dark in chromatin repair: repair of UV-induced DNA lesions by photolyase and nucleotide excision repair. *Embo J.*, 1999, **18,** 6585-6598.
43. W. Yang, Surviving the sun: Repair and bypass of DNA UV lesions. *Protein Sci.*, 2011, **20,** 1781-1789.
44. G. B. Sancar, DNA photolyases: Physical properties, action mechanism, and roles in dark repair. *Mutation Research*, 1990, **236,** 147-160.
45. A. Sancar, F. W. Smith and G. B. Sancar Purification of *Escherichia coli* DNA photolyase. *J. Biol. Chem.*, 1984, **259,** 6028-6032.
46. S. Bequer Urbano, V. H. Albarracin, O. F. Ordonez, M. E. Farias and H. M. Alvarez, Lipid storage in High-Altitude Andean Lakes extremophiles and its mobilization under stress conditions in *Rhodococcus* sp. A5, a UV-resistant actinobacterium. *Extremophiles,* 2013, **17,** 217-27.

Table and Figure captions

Figure captions

Figure 1. (A) Phylogenetic tree of putative photolyase sequences from *Acinetobacter* sp. Ver3 (Accession no. HQ443199) along with selected photolyases and related cryptochromes from NCBI database. (B) Sequence alignment between photolyases I from *E. coli* and Ver3Phr from *Acinetobacter* sp. Ver3. Secondary structure elements (arrows – beta sheets, columns – alpha helices) are shown above the alignment. Tryptophan residues from the typical triade are indicated as asterisks and are conserved at identical positions in the sequence. Residues in direct interaction with the FAD chromophore, labelled as diamonds, are fully conserved except for position 236 (arginine in the *E. coli* enzyme vs. glutamine-238 in Ver3Phr). Amino acids, interacting with the MTHF cofactor (arrowheads), are identical except for C292 (*E. coli*), which is changed into serine in Ver3Phr (S297).

Figure 2. Purification and spectroscopic analysis of Ver3Phr. (A). For purification, Ver3Phr was expressed in *E. coli* BL21 cells and purified to homogeneity, using affinity chromatography (Ni-NTA), followed by gel filtration (B). Western blot (C) clearly identified a band with an apparent molecular mass of ca. 60 kDa, which is in accord with the predicted mass of 54.7 kDa for His tag Ver3Phr. The ca. 25 KDa band, also detected by Western, may be due to partial degradation of the protein during purification and manipulation. The samples were analyzed by SDS-PAGE and Coomassie Blue staining. The mobility of molecular mass size markers (M), in kilodaltons, is indicated. Phr, photolyase.

Figure 3. (A) Absorbance spectra of "as-isolated" photolyases of VerPhr in comparison with EcPhr. The inset shows spectral zoom in the co-factor absorption region. For measurements, purified proteins were suspended in 50 mM Tris-HCl, 50 mM NaCl, 20% glycerol, 1 mM EDTA, 1 mM DTT-containing buffer (pH 7.5). (B) Excitation and emission fluorescence spectra of FAD (-·-·-·-), EcPhr (——) and Ver3Phr (——) obtained by setting emission and

excitation wavelengths at 520 nm and 440 nm, respectively. (C) Emission fluorescence spectra of (-·-·-·-), EcPhr (——) and Ver3Phr (——) obtained by UV excitation at 330 nm. All samples, including pure MTHF and FAD reference solutions, were prepared in buffer, pH 7.5 (in 50 mM Tris-HCl, 50 mM NaCl, 20% glycerol, 1 mM EDTA, 1 mM DTT).

Figure 4. Number of CPDs photoproducts produced in recombinant strains expressing the photolyases (EcPhr or Ver3Phr, respectively) compared with the untransformed recipient strain KY1225 (phr^- and RecA), and the control strain KY1056 (phr^+ and RecA) after UV-B exposure. Lesions are expressed as related with 10^6 pairs of the DNA extracted from the cell material after each treatment. The values of total photoproducts for the four strains are significatively different among them ($p < 0,05$).

Figure 5. Depletion of CPDs photoproducts from the tested strains after photo and dark-repairing assays, expressed as relative percentage of remaining photoproducts measured after UV5. Tested strains were untransformed recipient strain KY1225 (phr^- and RecA) or KY1225 expressing the photolyases (EcPhr and Ver3Phr), and the control KY1056 (phr^+ and RecA). Statistical analyses were performed between values of different treatments for the same strain (PR vs. DR). The values of total photoproducts for PR and DR treatments are significatively different among them ($p < 0,05$) for strain KY1225, KY1056 and KY1225 expressing Ver3Phr. For KY1225 expressing EcPhr, the values of total photoproducts for PR and DR treatments are not significatively different among them ($p < 0,05$).

Figure 6. Relative survival after UV-B exposure, photo and dark-repairing assays of recombinant strains expressing the photolyases (EcPhr and Ver3Phr) compared with the untransformed recipient strain KY1225 (phr^- and RecA) and the control strain KY1056 (phr^+ and RecA). **UV5**, Resulting population after 5 min of UV-B exposure. **DR**, UV-B exposed population allowed to dark-repair during 120 min. **PR**, UV-B exposed population allowed to photo-repair during 120 min. Non-exposed controls of all strain cultures plated at initial time

(T0) reached a mean value of 1.5 x10^6 UFC/ml (this is the 100% reference value). Percentages lower than 0.5% were computed as zero values in the graphic. Some treatments produce nule growth on agar plates (no UFC) even at the lowest dilution (10^{-1}). The detection limit was 1 x10^2 UFC/ml.

Statistical analyses were performed between values of UFC of different treatments for the same strain (PR vs. DR, UV vs. PR, UV vs. DR). The values are significatively different among them ($p < 0,05$) except for the following case: for KY1225 expressing EcPhr, the values for PR and DR treatments are not significatively different among them ($p < 0,05$). KY1225 and KY1056 were not subjected to statistical analyses, as most of the values were recorded as zero.

‡ Electronic supplementary information (ESI) available: Table S2 and Figures S1 and S3 and S4.

Figure S1. Western gel of recombinant cells carrying 1. pQE60Ver3Phr; 2. pQE60EcPhr; 3. pET52Ver3Phr; 4. pET28EcPhr superimposed with a graphic depicting density of each of the corresponding bands in Relative Density Units (See Material and Methods).

Table S2. The resulting peptides from the trypsin-digestion of ca. 60 kDa band were analysed by mass spectrometry (MALDI-TOF MS, Applied Biosystems Voyager-DE PRO, Foster City, USA) and the sequence of obtained peptides was matched with the predicted digested protein sequence using the Interactive FindPept analysis tool (http://web.expasy.org/tools/findpept/findpept-doc.html). User mass is the mass (daltons) of the peptides obtained after MALDI-TOF; DB mass is the mass of the peptide, including the post-translational and artefactual modifications (PTM), calculated from predicted digested protein sequence (Ver3Phr); **Δ**mass (daltons) is the difference in size from DBmass and User mass. Peptide gives the sequence in aminoacids of the peptidethe sequence of the peptide. The residues immediately before and after the sequence are indicated between round brackets but

not taken into account in the calculation. If either side of the peptide corresponds to a site of specific cleavage, it is denoted by a slash. Position is the position of the peptide in the sequence, supplied as the first and last residue. Modifications refer to the list of the PTMs applied to the peptide, in the order in which the underlined residues are indicated in the peptide sequence (http://web.expasy.org/findmod/findmod_masses.html). Missed cleavages are the number of missed cleavage sites within the sequence.

Figure S3. Multiple sequence alignment of the CPD-photolyase protein-coding gene from *Acinetobacter* sp. Ver3 (Acc. HQ443199) and closely related proteins within the crytochrome-photolyase family retrieved from public databases via the National Center for Biotechnology Information web site (www.ncbi.nlm.nih.gov). The alignment was carried out using ClustalW2 (http://www.ebi.ac.uk/Tools/clustalw2/index.html). After this alignment, a phylogenetic tree was built which is presented in Figure 1.

Figure S4. Absorption (black lines) and fluorescence emission (gray lines) spectra of a 20 μM MTHF solution: in water solution (dot lines) and in buffer 10 mM TRIS, 1 mM EDTA, 1 mM DTT and 20% v/v glycerol at pH 7.5 (solid lines).

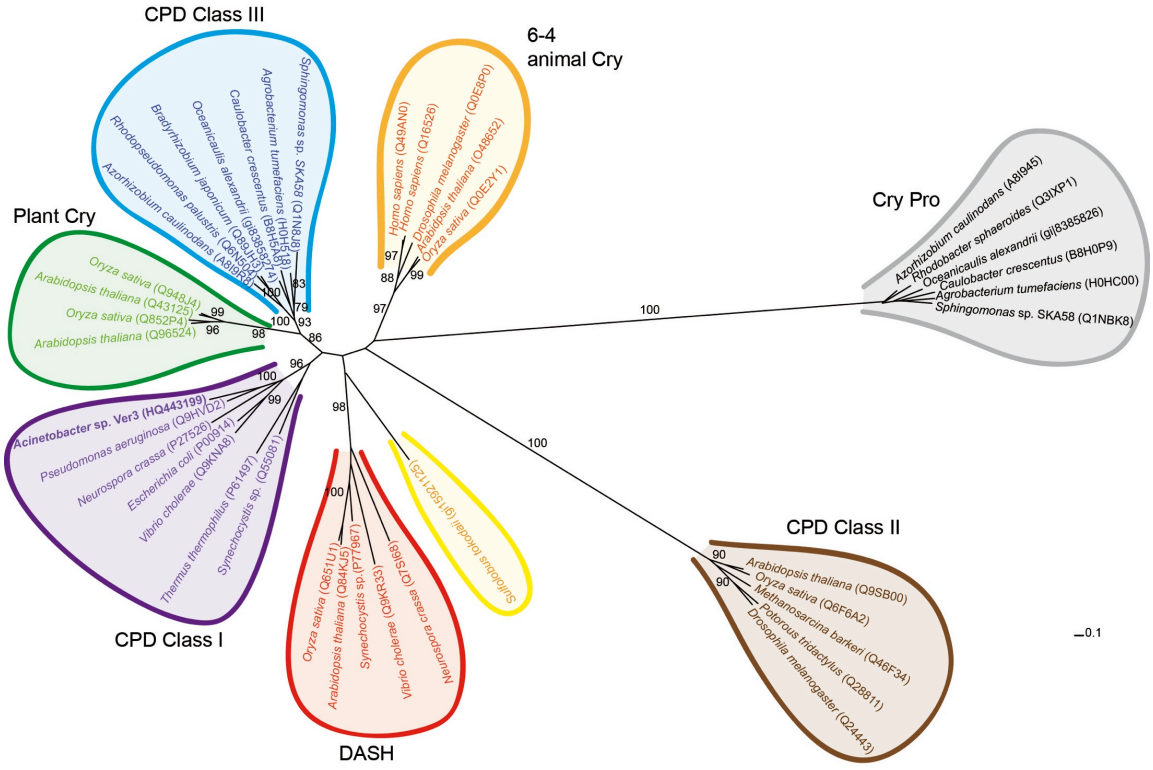

Fig. 1 (A)

1

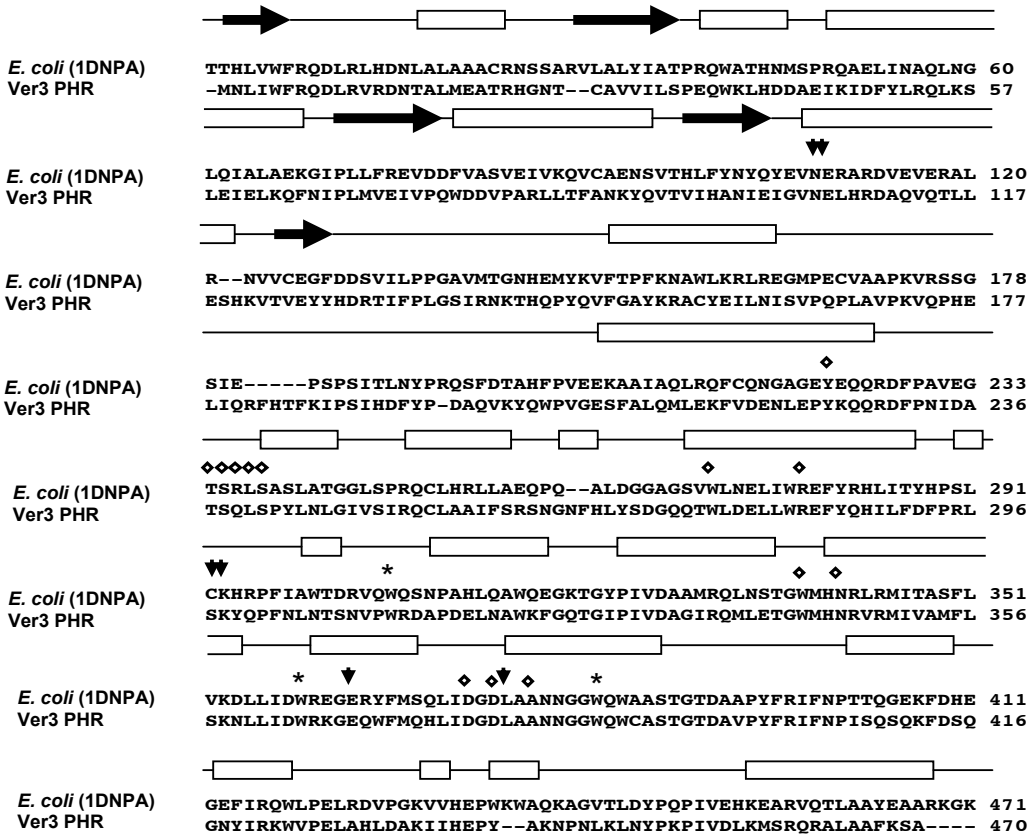

Fig. 1 (B)

2

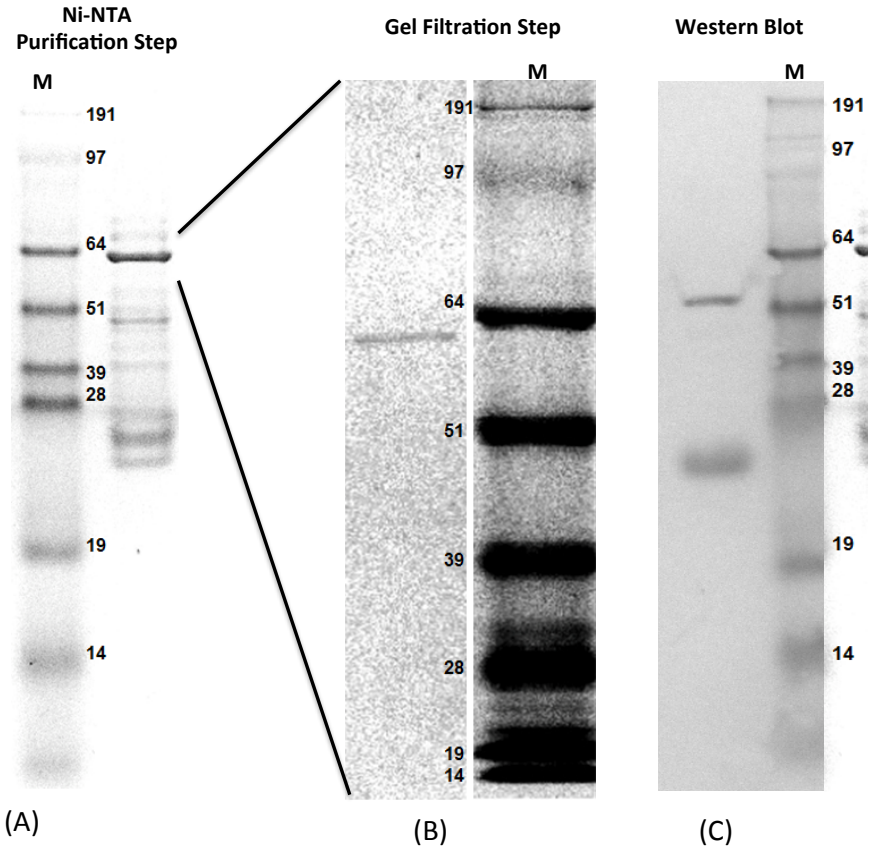

Fig. 2.

1

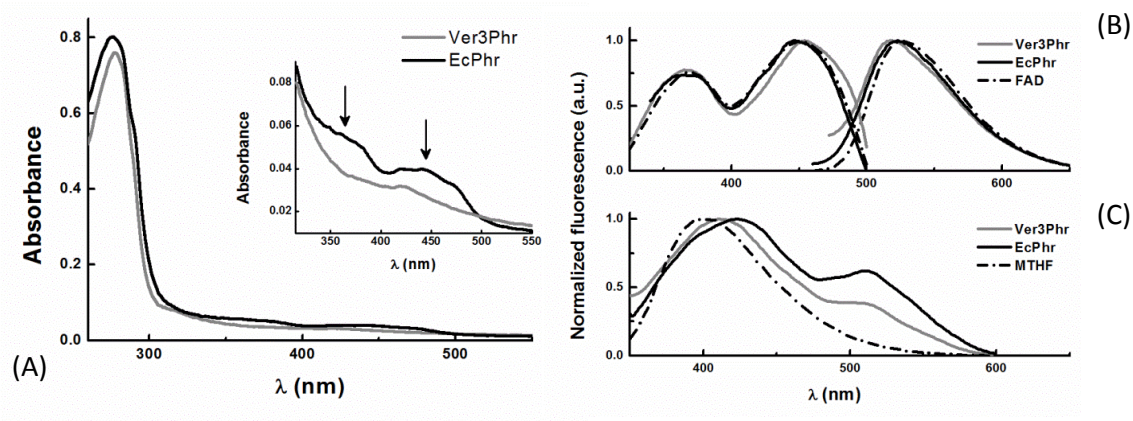

Fig. 3.

2

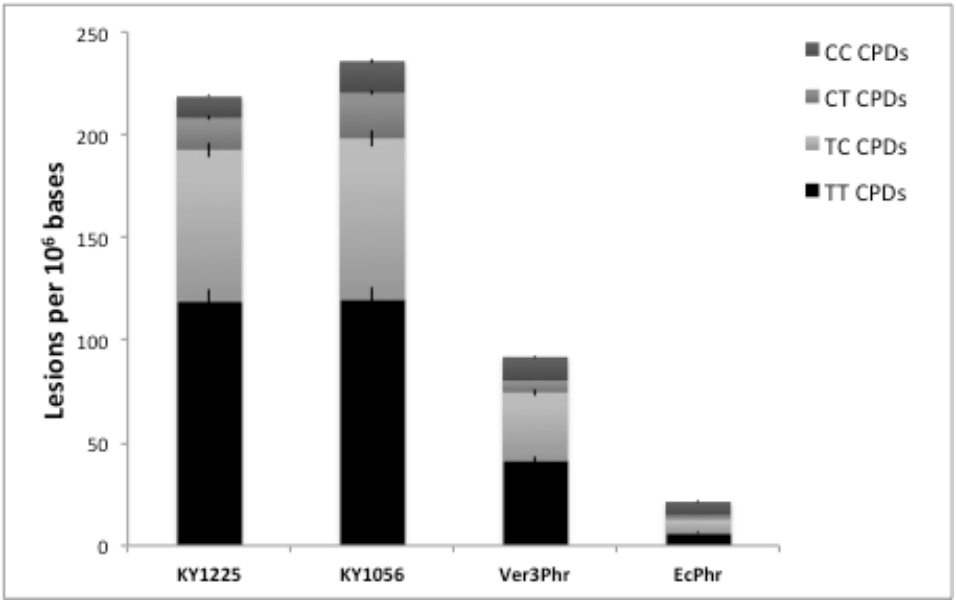

Fig. 4

1

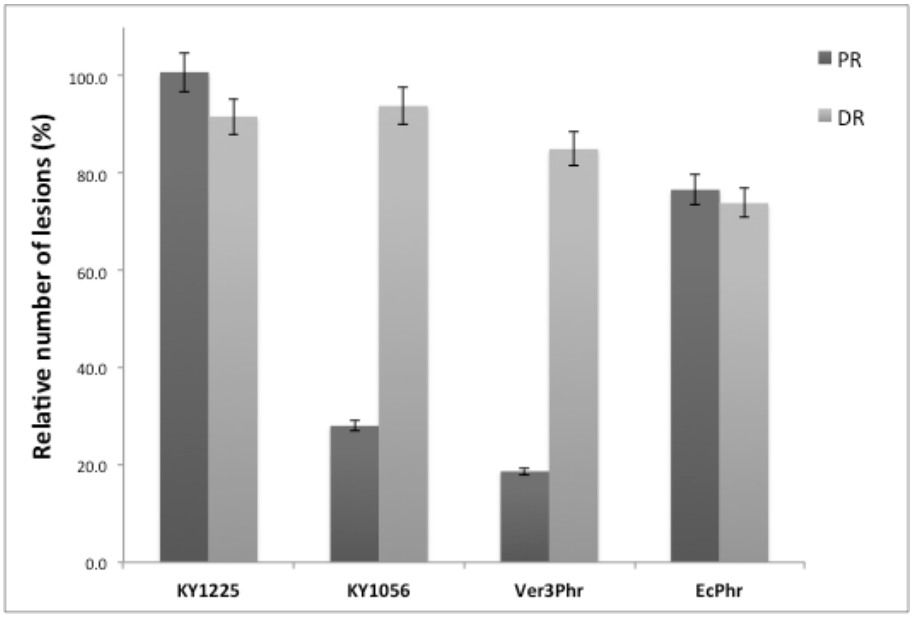

Fig. 5

2

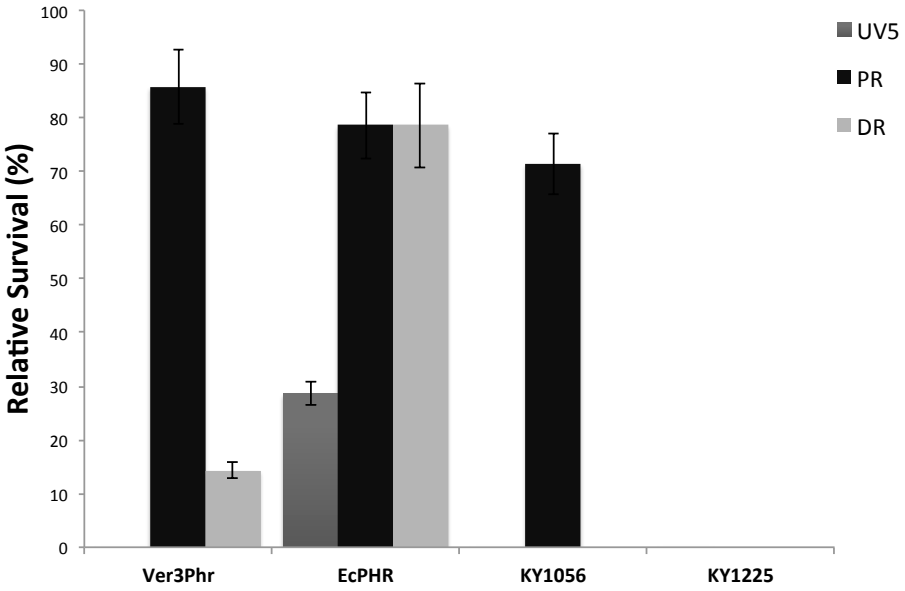

Fig. 6

1

2

1 Fig. S1

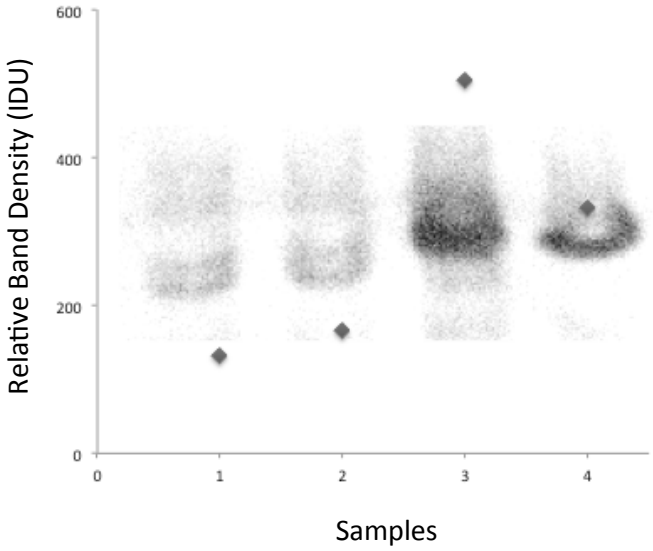

2

3

4 Table S2

	User mass	DB mass	Δmass (daltons)	peptide	position	modifications	missed cleavages
Matching peptides for specific cleavage:	1925.907	1925.947	0.039	(K)/YQWPVGESFALQMLEK/(F)	201-216	0	

	User mass	DB mass	Δmass (daltons)	peptide	position	modifications	missed cleavages
Matching peptides for unspecific cleavage:	1,526,505	1,526,837	0.331	(H)ILFDFPRLSKYQ(P)	289-300	1	
	1,526,505	1,526,884	0.378	(K)PIVDLKMSRQRAL(A)	452-464	2	
	1,526,505	1,526,894	0.389	(P)NLKLNYPKPIVDL(K)	444-456	0	
	1,566,581	1,566,755	0.173	(D)ENLEPYKQQRDF(P)	220-231	1	
	1,566,581	1,566,806	0.225	(N)KTHQPYQVFGAYK/(R)	141-153	1	
	1,599,489	1,599,849	0.359	(F)ANKYQVTVIHANIE(I)	88-101	0	
	1,599,489	1,599,937	0.447	(E)LIQRFHTFKIPSI(H)	178-190	1	
	1,655,536	1,655,919	0.382	(L)KQFNIPLMVEIVPQ(W)	63-76	0	
	1,690,409	1,690,728	0.318	(L)IDGDLAANNGGWQWCA(S)	376-391	0	
	1,690,409	1,690,849	0.440	(G)WMHNRVRMIVAMF(L)	343-355	1	
	1,722,683	1,722,885	0.201	(D)AQVKYQWPVGESFAL(Q)	197-211	0	

5

Matching peptides for unspecific cleavage:

User mass	DB mass	Δmass (daltons)	peptide	position	modifications	missed cleavages
1,722,683	1,722,907	0.224	(N)KTHQPYQVFGAYKR/(A)	141-154	2	
1,722,683	1,722,917	0.234	(H)LDAKIIHEPYAKNPN(L)	430-444	1	
1,722,683	1,722,917	0.234	(L)DAKIIHEPYAKNPNL(K)	431-445	1	
1,768,729	1,768,859	0.129	(K)/THQPYQVFGAYKRAC(Y)	142-156	1	
1,768,729	1,768,913	0.183	(S)QKFDSQGNYIRKWV(P)	411-424	2	
1,768,729	1,769,003	0.273	(E)LKQFNIPLMVEIVPQ(W)	62-76	0	
1,812,023	1,811,911	-0.111	(R)/EFYQHILFDFPRLS(K)	284-297	0	
1,812,023	1,811,944	-0.079	(D)FPRLSKYQPFNLNTS(N)	293-307	1	
1,850,311	1,849,933	-0.377	(D)FPNIDATSQLSPYLNLG(I)	231-247	0	
1,850,311	1,849,942	-0.369	(N)LLIDWRKGEQWFMQ(H)	360-373	1	
1,850,311	1,849,981	-0.330	(W)DDVPARLLTFANKYQV(T)	78-93	1	

Matching peptides for unspecific cleavage:

User mass	DB mass	Δmass (daltons)	peptide	position	modifications	missed cleavages
1,850,311	1,849,999	-0.311	(A)MFLSKNLLIDWRKGE(Q)	354-368	2	
1,850,311	1,850,007	-0.303	(Q)PHELIQRFHTFKIPS(I)	175-189	1	
1,893,488	1,893,049	-0.438	(K)/VQPHELIQRFHTFKI(P)	173-187	1	
1,893,488	1,893,096	-0.392	(S)VPQPLAVPKVQPHELIQ(R)	164-180	0	
1,968,243	1,968,013	-0.230	(W)REFYQHILFDFPRLS(K)	283-297	1	
1,990,409	1,990,003	-0.406	(L)LESHKVTVEYYHDRTI(F)	117-132	1	
1,990,409	1,990,003	-0.406	(Q)TLLESHKVTVEYYHDR/(T)	115-130	1	
1,990,409	1,990,003	-0.406	(T)LLESHKVTVEYYHDRT(I)	116-131	1	
1,990,409	1,990,102	-0.306	(K)/VQPHELIQRFHTFKIP(S)	173-188	1	
2,025,698	2,025,924	0.225	(F)MQHLIDGDLAANNGGWQW(C)	372-389	0	
2,025,698	2,025,962	0.264	(F)NLNTSNVPWRDAPDELNA(W)	303-320	0	

1

Matching peptides for unspecific cleavage:

User mass	DB mass	Δmass (daltons)	peptide	position	modifications
2,025,698	2,026,025	0.326	(R)/QDLRVRDNTALMEATRH(G)	8-24	2
2,025,698	2,026,050	0.352	(F)DSQGNYIRKWVPELAHL(D)	414-430	1
2,025,698	2,026,050	0.352	(D)SQGNYIRKWVPELAHLD(A)	415-431	1
2,087,768	2,087,993	0.225	(V)PWRDAPDELNAWKFGQTG(I)	310-327	1
2,087,768	2,088,062	0.293	(Q)TGIPIVDAGIRQMLETGWM(H)	326-344	0
2,087,768	2,088,106	0.337	(N)AWKFGQTGIPIVDAGIRQM(L)	320-338	1
2,108,572	2,108,092	-0.479	(S)QKFDSQGNYIRKWVPEL(A)	411-427	2
2,147,514	2,147,044	-0.469	(S)PEQWKLHDDAEIKIDFY(L)	35-51	1
2,147,514	2,147,067	-0.447	(S)KYQPFNLNTSNVPWRDAP(D)	298-315	1
2,147,514	2,147,070	-0.443	(R)/HGNTCAVVILSPEQWKLHD(D)	24-42	0
2,147,514	2,147,154	-0.359	(N)LIWFRQDLRVRDNTALM(E)	3-19	2
2,147,514	2,148,001	0.486	(G)WQWCASTGTDAVPYFRIF(N)	387-404	0
2,172,094	2,172,065	-0.029	(V)RDNTALMEATRHGNTCAVVI(L)	13-32	1
2,172,094	2,172,083	-0.010	(K)/YQWPVGESFALQMLEKFV(D)	201-218	0
2,172,094	2,172,192	0.098	(L)AHLDAKIIHEPYAKNPNLK/(L)	428-446	2
2,172,094	2,172,221	0.126	(S)QLSPYLNLGIVSIRQCLAAI(F)	239-258	0
2,172,094	2,172,229	0.134	(P)ARLLTFANKYQVTVIHANI(E)	82-100	1
2,214,483	2,214,115	-0.367	(S)FALQMLEKFVDENLEPYK/(Q)	209-226	1
2,214,483	2,214,128	-0.355	(K)/NLLIDWRKGEQWFMQHL(I)	359-375	1
2,214,483	2,214,239	-0.243	(A)HLDAKIIHEPYAKNPNLKL(N)	429-447	2
2,387,178	2,387,160	-0.017	(L)LIDWRKGEQWFMQHLIDGD(L)	361-379	1
2,387,178	2,387,160	-0.017	(L)IDWRKGEQWFMQHLIDGDL(A)	362-380	1
2,387,178	2,387,229	0.051	(W)REFYQHILFDFPRLSKYQ(P)	283-300	2
2,427,648	2,427,219	-0.429	(R)/DAPDELNAWKFGQTGIPIVDAGI(R)	313-335	0
2,427,648	2,427,230	-0.417	(C)ASTGTDAVPYFRIFNPISQSQK/(F)	391-412	1
2,427,648	2,427,234	-0.413	(D)LRVRDNTALMEATRHGNTCAVV(I)	10-31	2
2,427,648	2,427,234	-0.413	(L)RVRDNTALMEATRHGNTCAVVI(L)	11-32	2
2,427,648	2,427,263	-0.385	(E)IELKQFNIPLMVEIVPQWDD(V)	60-79	0
2,427,648	2,427,274	-0.373	(P)LMVEIVPQWDDVPARLLTFAN(K)	69-89	0
2,477,148	2,477,141	-0.007	(L)YSDGQQTWLDELLWREFYQ(H)	269-287	0
2,477,148	2,477,188	0.040	(S)DGQQTWLDELLWREFYQHI(L)	271-289	0

2

	User mass	DB mass	Δmass (daltons)	peptide	position	modifications	missed cleavages
Matching peptides for unspecific cleavage:							
	2,477,148	2,477,319	0.170	(P)QWDDVPARLLTFANKYQVTVI(H)	76-96		1
	2,638,363	2,638,497	0.133	(E)IKIDFYLRQLKSLEIELKQFN(I)	46-66		3
	2,638,363	2,638,497	0.133	(I)KIDFYLRQLKSLEIELKQFNI(P)	47-67		3
	2,775,702	2,775,353	-0.349	(W)FRQDLRVRDNTALMEATRHGNTCA(V)	6-29		3
	2,775,702	2,775,446	-0.255	(P)EQWKLHDDAEIKIDFYLRQLKS(L)	36-57		3
	2,775,702	2,775,556	-0.146	(L)DAKIIHEPYAKNPNLKLNYPKPIV(D)	431-454		2
	2,775,702	2,775,556	-0.146	(D)AKIIHEPYAKNPNLKLNYPKPIVD(L)	432-455		2
	2,826,595	2,826,374	-0.221	(S)IRQCLAAIFSRSNGNFHLYSDGQQT(W)	251-275		1
	2,826,595	2,826,421	-0.174	(F)RQDLRVRDNTALMEATRHGNTCAVV(I)	7-31		3
	2,881,893	2,881,419	-0.474	(A)LQMLEKFVDENLEPYKQQRDFPN(I)	211-233		2
	2,881,893	2,881,419	-0.474	(L)QMLEKFVDENLEPYKQQRDFPNI(D)	212-234		2
	2,881,893	2,881,463	-0.429	(R)/IFNPISQSQKFDSQGNYIRKWVPE(L)	403-426		2
	2,881,893	2,881,463	-0.429	(I)FNPISQSQKFDSQGNYIRKWVPEL(A)	404-427		2
	2,881,893	2,881,475	-0.418	(Q)TGIPIVDAGIRQMLETGWMHNRVRM(I)	326-350		2
	2,881,893	2,881,478	-0.415	(N)LGIVSIRQCLAAIFSRSNGNFHLYSD(G)	246-271		1
	2,881,893	2,881,495	-0.397	(L)TFANKYQVTVIHANIEIGVNELHRD(A)	86-110		1
	2,881,893	2,881,536	-0.357	(I)VPQWDDVPARLLTFANKYQVTVIHA(N)	74-98		1
	2,881,893	2,881,537	-0.356	(V)RMIVAMFLSKNLLIDWRKGEQWF(M)	349-371		3
	2,881,893	2,881,593	-0.299	(D)DVPARLLTFANKYQVTVIHANIEIGV(N)	79-104		1
	2,881,893	2,881,630	-0.263	(C)YEILNISVPQPLAVPKVQPHELIQR/(F)	157-181		1
	2,932,518	2,932,520	0.002	(Q)VQTLLESHKVTVEYYHDRTIFPLGS(I)	113-137		1
	2,932,518	2,932,667	0.149	(Q)PLAVPKVQPHELIQRFHTFKIPSIH(D)	167-191		2

1

	User mass	DB mass	Δmass (daltons)	peptide	position	modifications	missed cleavages
Potentially modified peptides, detected by mass difference and conforming to rules (considering only peptide masses that have not matched above):	2,537.90	1,941.94	-0.343	YQWPVGESFALQMLEK	201-216	1xTPO (THRX)	
	2,710.54	2,695.25	-0.281	SNGNFHLYSDGQQTWLDELLWR	262-283	1xTPO (DEAME)	

2

3

1 Fig. S3

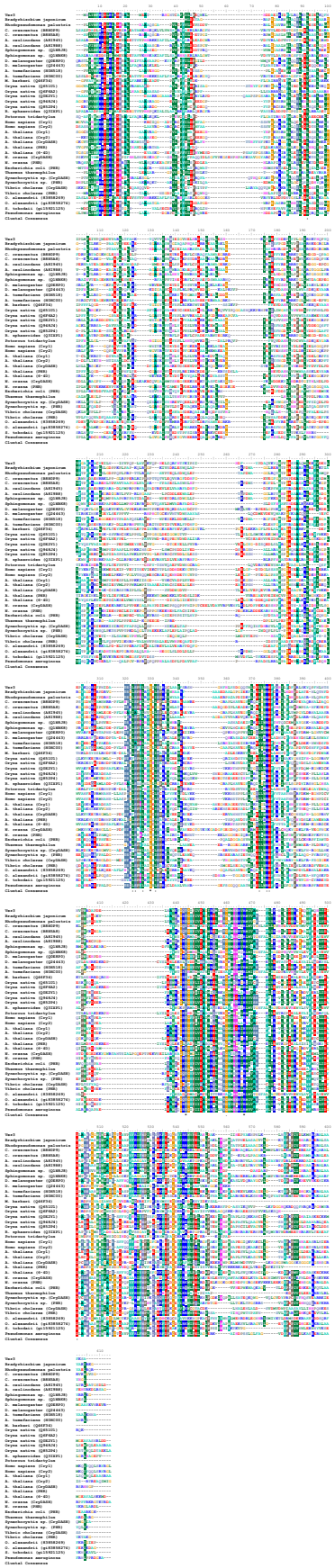

2

3

1 Fig. S4

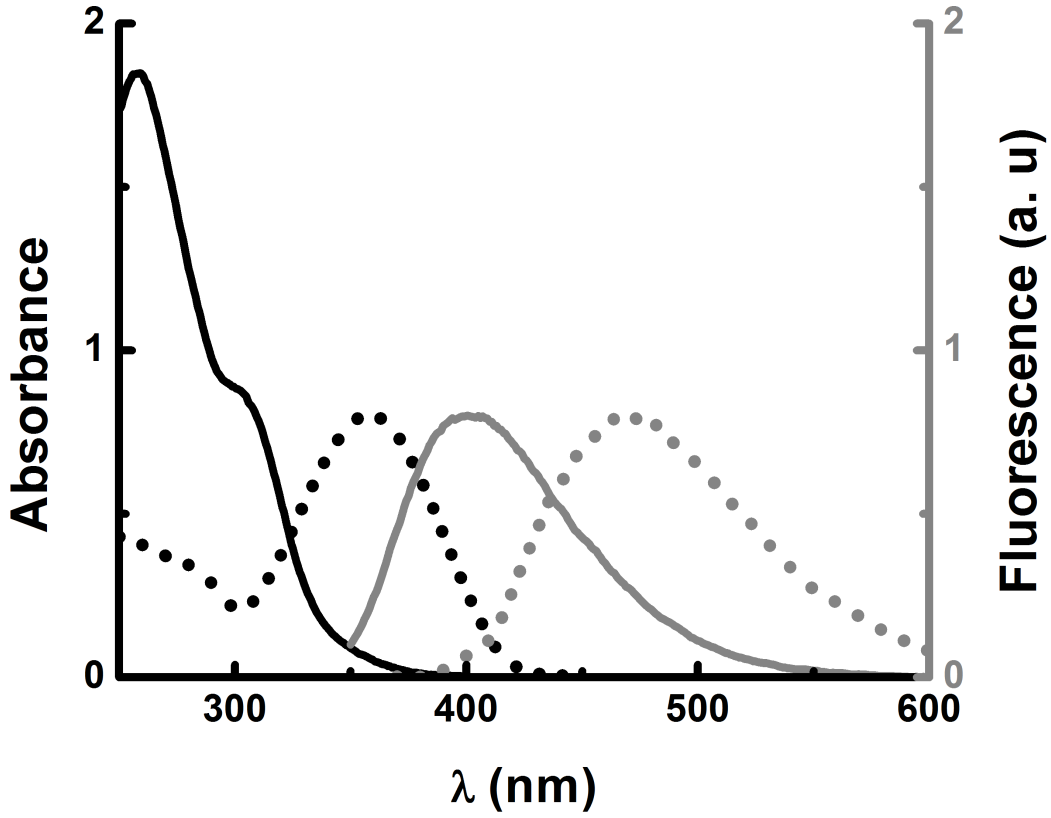

2